Study of Tire Noise Characteristics with High-Resolution Synchronous Images

Kuya Takami and Tomonari Furukawa
Mechanical Engineering Department, Virginia Polytechnic Institute and State University, USA.

Summary

This paper presents a paramtric study based on a high-resolution measurement system of rotating tires towards noise prediction. The developed system, to be mounted on a tire testing machine, consists of digital cameras, strobes, and a field-programmable gate array (FPGA) board. The developed system captures a clear instant image of a rotating tire irrespective of the rotation speed by triggering strobes. Since the rotation of a tire on a testing machine is periodic, the system can effectively capture the rotating tire at a high sampling frequency, though the digital cameras used may not have a high frame rate. The digital cameras proposed in the system are commercially available digital single-lens reflex (DSLR) cameras, which are CMOS-based and thus have high resolution, equipped with macro lenses, which further improve resolution by zooming into the tire deformation. This low-cost system is, therefore, considerably superior to high-speed cameras in both frame rate and resolution and can measure tire deformation associated with sound generation by synchronously measuring sound with a microphone array. The parametric study on a simple slot on a smooth tire was investigated by capturing images at every 0.025° tire rotation with synchronous microphone and spindle force measurements. The result demonstrated identification of the noise generation mechanism initiation timing and the characteristic of the noise.

PACS no. xx.xx.Nn, xx.xx.Nn

1. Introduction

Demands for noiseless tires have been increasing due to new regulations limiting pass-by noise in Europe and Japan. The noise generation and propagation have been extensively studied in the past few decades, which has resulted in the development of various modeling and simulation techniques. The computed sound, however, does not quantitatively match the experimentally measured sound [1, 2, 3]. This is partly because the noise is generated by multiple mechanisms and partly because it is propagated in a complicated manner. This gives rise to the need for synchronized high-resolution measurement of tire deformation, sound, and vibration. This enables validation of accuracy at every stage of noise prediction simulation.

Rotating tire noise can be generalized into structure-borne and air-borne noise. These noises are created by a complex interaction of both mechanical vibration and aerodynamic mechanisms. Modeling and simulation have been main methods of noise prediction. Larsson et al. [4] used a finite element model to investigate the dynamic behavior of the three dimensional tread block considering a frequency range of up to 3kHz. Other numerical models concentrate more on sound propagation processes such as the Biermann et al. [5] developed simulation process that evaluates a sound pressure field using a finite/infinite element approach. More recently, Brinkmeier et al. [6] have included more efficient numerical treatments for sound radiation prediction. Despite the afore mentioned development of techniques, the numerical prediction still lacks quantitative agreement with experimental results due to the complexity of noise generation and various physical phenomena that are not included in the models.

Contrary to modeling approaches, experimental methods include all of the noise generation mechanisms. Jochen [7] created miniature non-pneumatic tires to parametrically investigate noise characteristics based on groove geometry leading to a comparison to the Nilson [8] and Gogen [9] models. Cesbron et al. [10] focused on contact stress measurement using a smooth tire. Other experimental methods exist, however, most of the study does not synchronously capture the actual tire states and the timing of the noise generation.

A preliminary verification and validation study on the developed system under different operating conditions was demonstrated in [11], however, the study focused on image capture and did not analyze the sound data simultaneously. In addition, measurement of slot deformation with synchronous noise measurements at this resolution has not been achieved to the best of our knowledge.

This paper presents a parametric study of the simple tread tire noise generation with a high-resolution measurement system which quantifies tread deformation of fast-rotating tires using a CMOS-based digital single lens reflex (DSLR) camera, strobes, and a field programmable gate array (FPGA). The study shows the potential to reduce the discrepancy between analytical/numerical predictions and experimental observations by identifying and understanding specific noise generation mechanisms and their initiation timings.

This paper is organized as follows. The next section describes the developed system. The experimental setup and test procedure is described in Section 3 , followed by experimental results on tires with a simple two-dimensional tread geometry in Section 3.3. Finally, Section 4 summarizes conclusions and proposed future work.

2. Measurement System

The integrated system for rotating tire image and sound/spindle-force acquisition is used. Figure 1 shows the integrated data acquisition system, which consists of an FPGA controller, strobes, cameras, and a computer. The system is combined with an existing tire testing rig including a tire, rolling drum, drum controller, encoders, and data acquisition device. In the system, speed of the tire under test is indirectly regulated with a dedicated drum rotation speed controller. The tire spindle force, wheel position, and microphone array measurements are stored and processed with a data acquisition device. Only the wheel encoder signal is passed to the proposed system as a reference signal, providing data synchronization capability. The FPGA determines the wheel position from the reference signal, and captures tire deformation using strobe lights and cameras for offline analysis. Figure 2 shows an example of an FPGA development board.

3. Experimental Analysis

3.1. Test configuration

Figure 3 displays the parameters used to define slot dimensions. The slot was cut across the tire to meet the two dimensional assumption of the experiments. Additionally, tire shoulder material was removed to gain optical access. The single slot was introduced first, and then a second slot was added, creating a

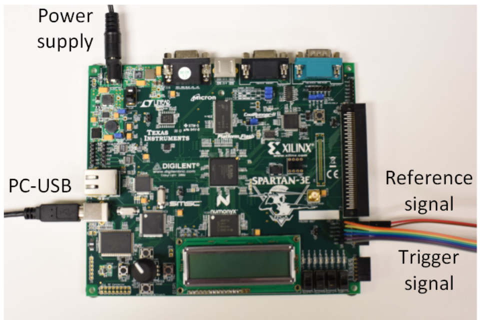

Figure 2. Visualization system implemented in a FPGA development board

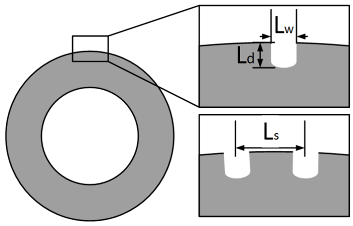

Figure 3. Tire slot dimensions

tread block. A slots spacing value, L_s, was selected based on common slot pitch values.

Figure 4 shows the microphone array placement around the rotating tire. As shown in the figure, the configuration was based on following the semi-anechoic chamber sound measurement specification on American National Standards S12.34. The yellow and green circles indicate far/near-field microphone positions, respectively, and all the microphone top-view and side-view dimensions are specified in the figure.

3.2. Procedure

All the tire experiments are performed in a semi-anechoic chamber shown in the Figure 5. The microphone array and the spindle-force load cell readings are collected simultaneously to correlate noise generation initiation and physical mechanisms. The 10 ft diameter drum and 215/60R16 tire, strobes, and a camera were used for the setup. Figure 6 shows a hand-cut plain tread tire, with a two-dimensional design, to simplify and separate noise generation mechanisms and reduce the complexity of the tire tread design. The tire tread shoulder was cut to expose the tread side view and minimize additional noise generation. All the data was collected in a single tread slot with a secondary slot introduced later to study the resultant interference of the noise and the change in structural behavior. The capability of the developed system was

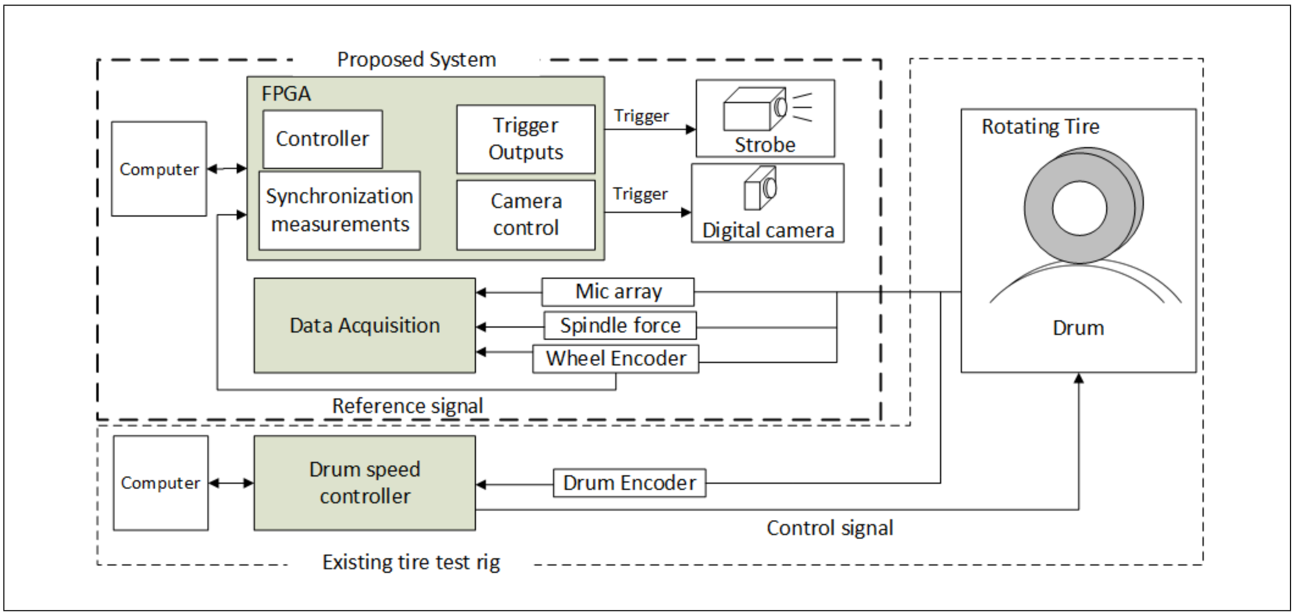

Figure 1. Overall system schematic

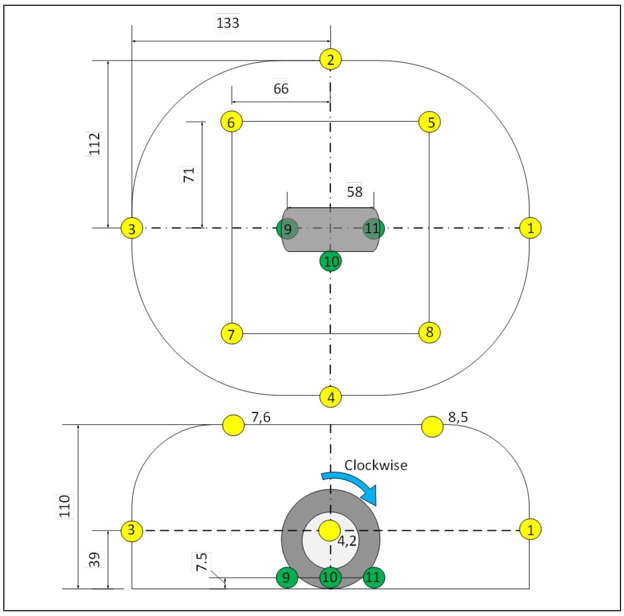

Figure 4. Microphone placement in centimeter

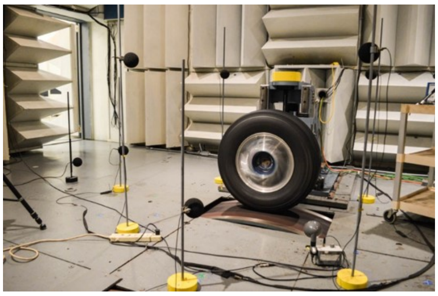

Figure 5. Semi-anechoic chamber testing facility

Figure 6. Hand cut tire with two slots

examined using multiple operating conditions, which are listed on Table I.

3.3. Results

Figure 7 shows an example of the synchronous microphone and tire slot image captured through the contact patch with the tire rotating in a counterclockwise direction. Microphone pressure signals for leading edge,mic 9, and trailing edge, mic 11, are shown relative to the tire position. The images were captured at every 0.025°increment. Thus, the position range of 35°shown in the figure contains 1400 images. The acoustic signal plot is labeled at four different positions indicating the corresponding tire position shown in the tire images. The slot dimension {5mm, 7mm} at three different speeds rotating in a counterclockwise direction are further studied.

3.3.1. Leading edge

Figure 8(a) shows normalized leading edge mic 9 measurements at different speeds. The figure shows that dominant frequency does not change when the speed

Table I. Dimensions and other parameters for the experiments.

Parameter	Value
Encoder	3600 [PPR]
Tire type	215/60R16
Inflation pressure	35 [PSI]
Load	1000 [lb]
Direction	Clockwise/ Counterclockwise
Speed	40, 60, 80 [km/h]
Slot width	140 [mm]
$\{L_w, L_d\}$	$\{5,5\}, \{5,7\}, \{10,5\}$ [mm]
L_s	30 [mm]
Analog sample rate	88.2 [kHz]
Strobe duration (⅓ peak value)	1.2 [µs]

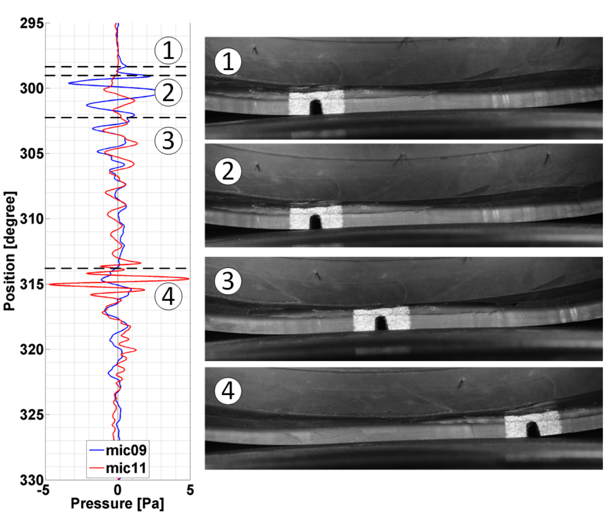

Figure 7. Synchronous image and microphone data

of the tire is varied. This is also confirmed from the spectrogram results in Figure 10 demonstrating that the maximum value of the leading edge signal stays in 1050 $\sim$ 1150Hz range. The signal shape characteristics are qualitatively similar at different speeds. However, the subtle differences can be observed such as a couple of initial peaks of sound signal corresponding to the first and second edge engagement as shown in Figure 8(b). The first peak identifies tire position when the first edge of the slot is in contact with the drum surface and the second peak identifies the second edge engaging the drum depicted in the Figure 9. Commonly the second edge engagement is referred to as impact noise. The peak time differences, which directly correspond to the dimension of L_w, are calculated to be $\{4.4, 4.5, 4.8\}$ millimeters.

3.3.2. Trailing edge

Figure 11(a) shows the normalized trailing edge mic 11 measurements at different speeds. Unlike the observation for the leading edge, there is a change in pressure before the dominant wave that results from

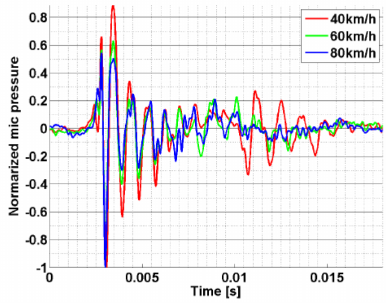

(a) Leading edge

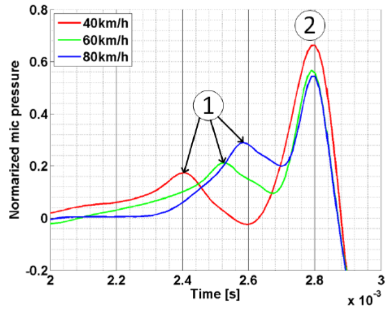

(b) First peak zoomed view

Figure 8. Normalized leading edge Mic 9

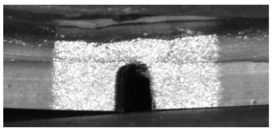

(a) $\theta = 297.00$

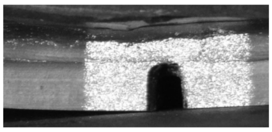

(b) $\theta = 297.75$

Figure 9. Leading edge slot position

the leading edge noise generation. In addition, the trailing edge shows the frequency change in resulting noise where a higher speed leads to a higher frequency. The shape of the dominant signal is similar at different speeds as seen in the zoomed section of the plot in Figure 11(b), however, the dominant frequency value increases. The dominant frequency increase can be also confirmed in the spectrograms in Figure 12 where the maximum frequency is higher and has a wider frequency range than the leading edge. Another major difference between the leading and trailing edge signals is the duration of the wave generated by the event. For this example, the trailing edge noise duration is 35% less than that of the leading edge.

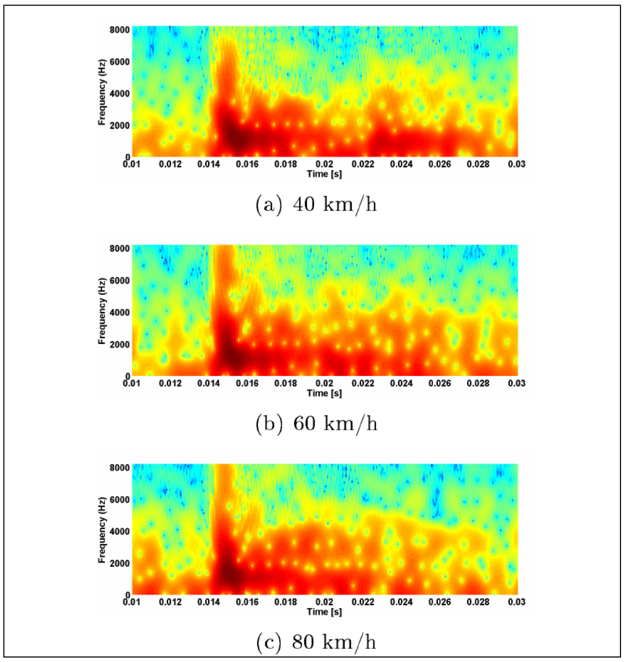

(a) 40 km/h

(b) 60 km/h

(c) 80 km/h

Figure 10. Normalized spectrogram of mic 9

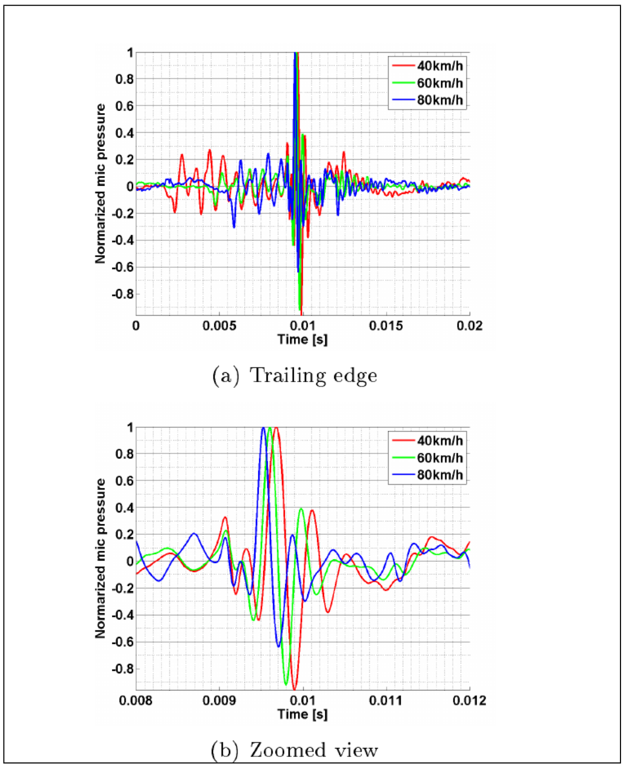

(a) Trailing edge

(b) Zoomed view

Figure 11. Normalized trailing edge mic 11

4. Conclusion

This paper has described the simple tread parametric study based on the high-resolution measurement system. High-resolution images with synchronous data acquisition identify specific noise generation mechanisms and their initiation timings. The simultaneous

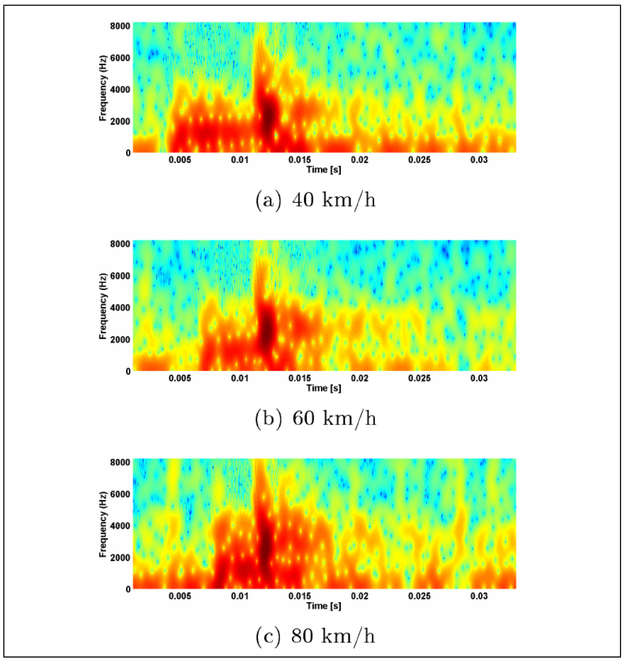

(a) 40 km/h

(b) 60 km/h

(c) 80 km/h

Figure 12. Normalized spectrogram of mic 11

tire slot image with a microphone array and spindle force measurements allow a strong correlation between signal peaks and slot engagement. Separation of the slot's initial and secondary edges was identified with the frequency characteristics of the signals.

Future work will involve using this system to collect extended datasets with more realistic tread shapes. In addition, instead of a hand-cut slot, the geometry can be more consistently created using a laser tire cutter with different geometry dimensions. Furthermore, the finite element simulation should be incorporated with these measurements to validate the numerical estimation of the tread deformation.

Acknowledgements

This work was primarily supported by Center for Tire Research (CenTiRe), an Industry/University Cooperative Research Centers Program supported by National Science Foundation. The research center led by Virginia Tech and cooperated with the University of Akron. All the rolling tire experiment were performed at Bridgestone Americas, Inc. located in Akron Ohio.

References

[1] Ulf Sandberg and Jerzy A Ejsmont. *Tyre/road noise reference book*. 2002.

[2] DJ O'Boy and AP Dowling. Tyre/road interaction noise-numerical noise prediction of a patterned tyre on a rough road surface. *Journal of Sound and Vibration*, 323(1):270–291, 2009.

[3] Mir Hamid Reza Ghoreishy. A state of the art review of the finite element modelling of rolling tyres. *Iranian Polymer Journal*, 17(8):571–597, 2008.

[4] Krister Larsson, Stephane Barrelet, and Wolfgang Kropp. The modelling of the dynamic behaviour of tyre tread blocks. *Applied Acoustics*, 63(6):659–677, 2002.

[5] Jan Biermann, Otto von Estorff, Steffen Petersen, and Holger Schmidt. Computational model to investigate the sound radiation from rolling tires 5. *Tire science and technology*, 35(3):209–225, 2007.

[6] Maik Brinkmeier and Udo Nackenhorst. An approach for large-scale gyroscopic eigenvalue problems with application to high-frequency response of rolling tires. *Computational Mechanics*, 41(4):503–515, 2008.

[7] Jochen Eisenblaetter. *Experimental investigation of air related tyre/road noise mechanisms*. PhD thesis, © Jochen Eisenblaetter, 2008.

[8] N.-A Nilsson. Possible methods of reducing external tyre noise. pages 247–259, 1979.

[9] MJ Gagen. Novel acoustic sources from squeezed cavities in car tires. *The Journal of the Acoustical Society of America*, 106(2):794–801, 1999.

[10] Julien Cesbron, Fabienne Anfosso-Ledee, Denis Duhamel, Hai Ping Yin, and Donatien Le Houedec. Experimental study of tyre/road contact forces in rolling conditions for noise prediction. *Journal of sound and vibration*, 320(1):125–144, 2009.

[11] Kuya Takami and Tomonari Furukawa. High-resolution deformation measurement system for fast rotating tires. In *ASME 2015 International Design Engineering Technical Conferences and Computers and Information in Engineering Conference*. American Society of Mechanical Engineers, 2015 submitted.